PNAS RESEARCH ARTICLE | APPLIED BIOLOGICAL SCIENCES OPEN ACCESS

eIF4A controls translation of estrogen receptor alpha and is a therapeutic target in advanced breast cancer

Jacob A. Boyer[a,b,c], Ezra Y. Rosen[d], Malvika Sharma[b], Madeline A. Dorso[e], Nicholas Mai[d], Corina Amor[a,f], Jason M. Reiter[b], Ram Kannan[f], Sunyana Gadal[b], Jianing Xu[b], Matthew Miele[g], Zhuoning Li[g], Xiaoping Chen[h], Qing Chang[h], Fresia Pareja[i], Stephan Worland[i], Douglas Warner[i], Sam Sperry[j], Gary G. Chiang[j], Peggy A. Thompson[j], Guangli Yang[k], Ouathek Ouerfelli[k], Alexander Drilon[d], Elisa de Stanchina[h], Hans-Guido Wendel[f], Sarat Chandarlapaty[d,e,l,1], and Neal Rosen[b,d,l,1]

Affiliations are included on p. 10.

Edited by Myles Brown, Dana-Farber Cancer Institute, Boston, MA; received November 26, 2024; accepted June 4, 2025

Most breast cancers depend on hormone-stimulated estrogen receptor alpha (ER) activity and are sensitive to ER inhibition. Resistance can arise from activating mutations in the gene encoding ER (*ESR1*) or from reactivation of downstream targets. Newer ER antagonists occasionally show efficacy but are largely ineffective as single agents in the long term. Here, we show that ER translation is eIF4E/cap-independent yet sensitive to inhibitors of the translation initiation factor eIF4A. EIF4A inhibition reduces the expression of ER and cell cycle regulators such as cyclin D1. This leads to growth suppression in ligand-independent breast cancer models, including those driven by ER mutants and fusion proteins. Efficacy is enhanced by adding the ER degrader, fulvestrant. The combination further lowers ER expression and blocks tumor growth in vitro and in vivo. In an early clinical trial (NCT04092673), the eIF4A inhibitor zotatifin was combined with either fulvestrant or fulvestrant plus CDK4 inhibitor, abemaciclib, in patients with acquired resistance to these agents. Multiple clinical responses including a handful of durable regressions were observed, with little toxicity. Thus, eIF4A inhibition could be useful for treating ER+ breast cancer resistant to other modalities.

estrogen receptor | eIF4A | translation | breast cancer | zotatifin

Significance

This work identifies eIF4A as a major regulator of both estrogen receptor (ER) translation and breast cancer growth. We demonstrate that eIF4A is required to maintain ER expression and expression of cell cycle regulators such as cyclin D1 and CDK4. EIF4A inhibitors, especially when combined with selective estrogen receptor degraders (SERDs) such as fulvestrant can treat metastatic breast cancer in vitro, in vivo, and in patients.

Estrogen receptor alpha (ER) is a member of the extended family of nuclear receptors (1). Upon estrogen binding, ER translocates to the nucleus, dimerizes, and induces the transcription of an ensemble of genes involved in proliferation, lineage specification, and other functions (2). ER is required for development of the mammary ductal epithelium and 70 to 75% of breast tumors retain dependence on ER for growth (3, 4). Hormonal therapies targeting ER are active in these ER+ metastatic breast cancers and have been remarkably successful in improving outcomes. Unfortunately, resistance to hormonal therapy is nearly universal, and over 90% of patients develop resistance to various drugs targeting ER (5). Dysregulation of the PI3K/AKT/mTOR pathway is common in ER-dependent breast cancer, and activating mutations of *PIK3CA*, the catalytic subunit of class 1 PI3 Kinase, occur in 40% of these tumors (6–8). The PI3K pathway enhances the proliferation, motility, and invasiveness of these tumor cells and activation of the mTOR complex 1 (mTORC1) maintains high levels of eIF4E-dependent protein translation (9, 10). Combination PI3K/ER inhibition is a clinically effective strategy but its effects are lessened by enhanced ER expression and signaling following PI3K inhibition (11, 12). Inhibition of mTORC1 decreases total protein translation by as much as 70% (13). However, for a number of short lived-proteins, expression can be maintained using noncanonical mechanisms of protein translation (10, 14–16). Prior studies have estimated that ER is a short-lived protein with a half-life of approximately 3 to 6 h (17). We therefore asked how ER expression is maintained when PI3K/mTOR is inhibited. We found that ER expression is maintained during mTOR inhibition by an eIF4E/cap-independent translation mechanism that depends on the 5' untranslated region (5' UTR) of the mRNA encoding ER (*ESR1*). EIF4E-independent ER translation is instead dependent on the RNA helicase eIF4A, a different component of the eIF4F complex. Pharmacological inhibition of eIF4A reduces the expression of ER as well as a number of short half-life proteins controlling cell cycle entry including cyclin D1, cyclin D3, and CDK4. EIF4A inhibitors effectively reduce ER expression and block the growth of ER-dependent tumor models driven by wild type ER, hormone-insensitive ER mutants, and ER fusion proteins. Moreover, inhibition of ER translation via eIF4A blockade combined with induction of ER degradation by the ER degrader fulvestrant powerfully suppresses ER expression and inhibits the growth of breast tumor xenograft models. This strategy has been investigated in an early

Author contributions: J.A.B., E.Y.R., M.A.D., N.M., C.A., J.X., S.S., E.d.S., H.-G.W., S.C., and N.R. designed research; J.A.B., E.Y.R., M.S., M.A.D., N.M., C.A., J.M.R., S.G., J.X., M.M., Z.L., X.C., Q.C., F.P., and A.D. performed research; J.A.B., E.Y.R., R.K., S.G., S.W., D.W., S.S., G.G.C., P.A.T., G.Y., O.O., H.-G.W., and S.C. contributed new reagents/analytic tools; J.A.B., E.Y.R., M.S., M.A.D., N.M., C.A., J.M.R., R.K., S.G., J.X., S.C., and N.R. analyzed data; and J.A.B., E.Y.R., M.S., R.K., S.C., and N.R. wrote the paper.

Competing interest statement: S. Chandarlapaty previously owned equity in and received personal fees from effector therapeutics. Neal Rosen was on the scientific advisory board (SAB) and previously owned equity in Effector. Neal Rosen and S. Chandarlapaty previously owned equity in effector therapeutics.

This article is a PNAS Direct Submission.

[1]To whom correspondence may be addressed. Email: chandarS@mskcc.org or rosenn@mskcc.org.

This article contains supporting information online at https://www.pnas.org/lookup/suppl/doi:10.1073/pnas.2424286122/-/DCSupplemental.

Published July 21, 2025.

phase clinical trial (NCT04092673) that combines the eIF4A inhibitor, zotatifin with fulvestrant, with or without the CDK4 inhibitor, abemaciclib. Early data suggest that this combination is well tolerated (18)and multiple tumor regressions have been observed in heavily pretreated endocrine therapy resistant patients (18).

Results

ER Expression Is eIF4A Dependent. Canonical eukaryotic translation is initiated by eukaryotic initiation factor 4E (eIF4E), which upon binding the m7G mRNA cap, nucleates the initiation complex eIF4F (19, 20), composed of eIF4E, eIF4G, and eIF4A. Transcripts whose translation are eIF4E and eIF4G dependent are often referred to as "cap-dependent," whereas eIF4A can participate in both "cap-dependent" and "cap-independent" translation (21). mTORC1 controls translation initiation by phosphorylating and preventing the binding of the inhibitor 4EBP1 to eIF4E (13, 22). Ribosome scanning and prescanning remodeling within the 5' UTR are facilitated by the DEAD-box RNA helicase eIF4A, which unwinds structured RNAs (23, 24) (Fig. 1*A*). Inhibitors of mTORC1 cause dephosphorylation of 4EBP1, promoting its binding to eIF4E and reducing global protein synthesis. Some transcripts, often termed "cap-independent," remain insensitive and continue to be translated when mTORC1 is inactive (13, 25, 26). Since ER expression increases following PI3K/mTOR inhibition (11, 12) we hypothesized that ER translation is cap/eIF4E-independent. To test this, we treated ER+ breast cancer cell line MCF7 with the potent mTORC1/2 inhibitor, RapaLink-1 (27) (Fig. 1*B*). MTOR substrates, AKT, S6, and 4EBP1, were dephosphorylated by 4 h post treatment, and this inhibition was accompanied by a reduction in global protein synthesis of up to 75% as measured by puromycin incorporation (Fig. 1*B* and *SI Appendix,* Fig. S1*A*). 4EBP1 dephosphorylation was associated with enhanced interaction of 4EBP1 with eIF4E while reducing the interaction between eIF4E and eIF4G (Fig. 1*B*). Dephosphorylation of 4EBP1 was also associated with a reduction in cyclin D1, translation of which is known to be mTOR/eIF4E dependent (28, 29) (Fig. 1*B*). In contrast to cyclin D1, ER levels were unchanged when global and cap-dependent translation were reduced by the drug (Fig. 1*B*). Similar results were obtained in other luminal breast cancer cell lines, T47D and ZR-75-1 treated with RapaLink-1. (*SI Appendix*, Fig. S1*B*). In contrast to mTOR inhibition, blocking all mechanisms of protein translation with cycloheximide resulted in a time-dependent decrease of ER expression, which had a half-life between 4 and 8 h (*SI Appendix*, Fig. S1*C*). mTOR regulates translation via substrates LARP1, S6K, and 4EBP1, but only 4EBP1 directly engages eIF4E (13, 30). Using L-azidohomoalanine (AHA labeling to measure translation directly (31), we confirmed ER translation was eIF4E independent by expressing doxycycline-inducible, constitutively active 4EBP1 ("4A" mutant: T37A/T46A/S65A/T70A) (32). Increasing mutant expression dose-dependently suppressed cap-dependent translation and cyclin D1 synthesis but did not affect ER or MYC, the latter of which is known to be translated independently of eIF4E (33, 34) (Fig. 1*C* and *SI Appendix*, Fig. S1*D*). Cap-independent translation is often mediated by internal ribosome entry sites (IRES) within mRNA 5' UTRs (15, 16, 33, 35). Using a bicistronic luciferase reporter assay (36), we demonstrated the *ESR1* 5' UTR significantly drives cap-in-dependent translation, ~120-fold higher than empty vector and 5 fold higher than the poliovirus IRES positive control, but lower than that of a powerful IRES from the *Myc* 5' UTR (Fig. 1*D*). We confirmed that the cap-independent activity of the *ESR1* 5' UTR was not an artifact of cryptic promoter activity or transcriptional read-through by using luciferase assay constructs containing the *ESR1* 5' UTR with a hairpin and lacking a promoter (*SI Appendix*, Fig. S1*E*). These results reveal that while ER is a short-lived protein, its translation can be sustained in an eIF4E independent manner during mTOR inhibition, and this eIF4E-independent activity is mediated through elements in the 5' UTR. IRES elements in the mRNA 5' UTR often have complex secondary structures that bind to a subset of eukaryotic initiation factors that recruit the ribosome. Such structures are remodeled or unwound by RNA helicases during initiation (37, 38). We hypothesized that eIF4A, the major RNA helicase employed in translation initiation, might control ER protein synthesis. We treated MCF7 with 20 nM of the selective (39) eIF4A inhibitor silvestrol and observed a time-dependent decrease in ER expression, beginning at 4 h and continuing up to 48 h (Fig. 1*E*). Similar reductions in ER protein expression were observed in four other cell lines treated with silvestrol (*SI Appendix*, Fig. S1*F*). In addition to being eIF4E dependently translated, cyclin D1 translation has also been shown to be eIF4A dependent (40, 41). Both silvestrol and its synthetic rocaglate analog CR-31-B (42) inhibited ER and cyclin D1 expression at concentrations from 20 to 30 nM at 24 h. (*SI Appendix*, Fig. S1*G*). We observed a time-dependent potency effect on ER expression when cells were treated with silvestrol (*SI Appendix*, Fig. S1*H*). ER expression was inhibited approximately as well with 5 nM silvestrol at 72 h. as 20 nM at 24 h (*SI Appendix*, Fig. S1*H*). Two other mechanistically distinct inhibitors of eIF4A, pateamine A and hippuristanol (43, 44), also inhibited both ER and cyclin D1 expression by 24 h (*SI Appendix*, Fig. S1*I*). Again using AHA labeling, we found that the translation of cyclin D1 but not of ER was suppressed by mTOR inhibition, whereas the translation of both cyclin D1 and ER were reduced in the presence of either silvestrol or cycloheximide (Fig. 1*F*). Genetic knockdown confirmed that only eIF4A1 depletion significantly reduced ER protein, while consistent with its cap-dependent translation, knockdown of any eIF4F component reduced cyclin D1 (*SI Appendix*, Fig. S1*J*). *ESR1* mRNA levels were largely stable during the first 24 h post silvestrol treatment, decreasing at most by 25% during the first 16 h, implying a posttranscriptional mechanism of ER regulation by eIF4A (*SI Appendix*, Fig. S1*K*) Finally, we tested whether eIF4A inhibition reduces the cap-independent translation driven by the *ESR1* 5' UTR. As a function of dose, silvestrol effectively blocked the cap-independent translation mediated by the 5' UTR of *ESR1* (Fig. 1*G*). By inhibiting cap-dependent translation, while leaving the ESR1 5'UTR-driven cassette unaffected, the mTOR inhibitor MLN0128 increased the firefly/renilla ratio as a function of dose (Fig. 1*G*). Taken together, these results establish that ER is translated in an eIF4A-dependent but eIF4E-independent manner and is therefore cap-independent, while cyclin D1 translation depends on eIF4E, eIF4G, eIF4A and is therefore cap-dependent.

eIF4A Regulates ER Activity and Cell Growth. In MCF7 cells treated with 20 nM silvestrol for 24 h, expression of ER-regulated genes (*PGR, GREB1, TFF1, IGFBP4,* and *SERPINA1*) was decreased, and that of an ER-repressed gene *TP53IN1* was increased (Fig. 2*A*) (45). Silvestrol also blocked estradiol-stimulated gene expression in MCF7 and T47D cells (Fig. 2*B* and *SI Appendix*, Fig. S2*A*). We performed chromatin immunoprecipitation of ER bound to an estrogen response element (ERE) in target gene *TFF1/pS2*. Silvestrol pretreatment reduced ER occupancy of this response element by approximately 2.5-fold and prevented the estradiol-induced ER occupancy at this site by a similar magnitude (Fig. 2*C*). Thus, eIF4A inhibition reduced the levels of ER at its enhancer elements, and thus its ability to transactivate target gene

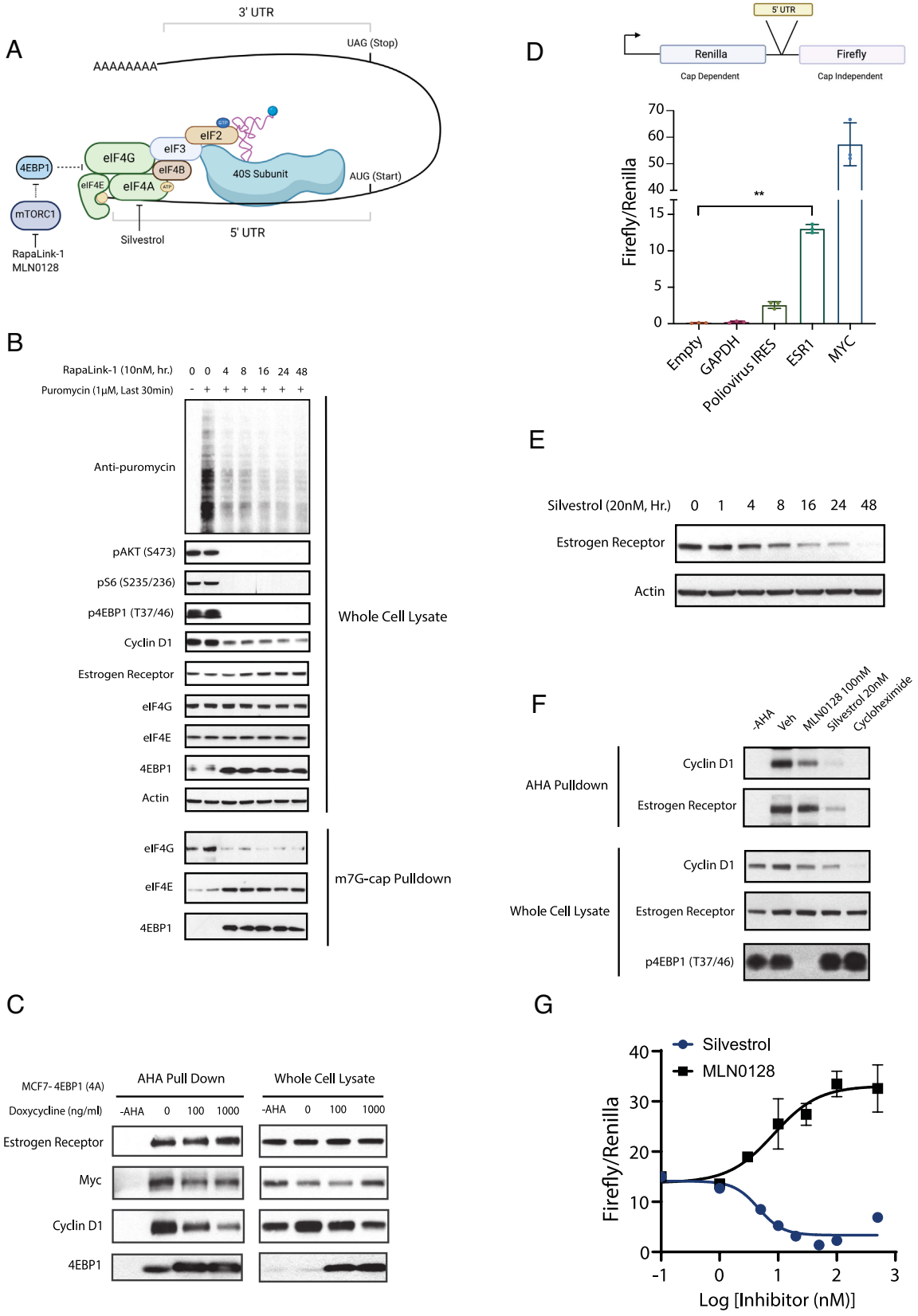

Fig. 1. Estrogen receptor alpha (ER) expression is eIF4A dependent. (*A*). Schematic of eukaryotic translation initiation. The eIF4F complex is depicted in green. (*B*). MCF7 cells were treated with 10 nM RapaLink-1 for the indicated times. To measure global translation, 1 μM puromycin was pulsed for the last 30 min, and incorporation was assessed using an antipuromycin antibody. For m7G cap pulldowns, 200 μg of cell lysate was incubated with m7G conjugated sepharose to precipitate the eIF4F complex. (*C*). MCF7 cells expressing doxycycline inducible 4EBP1-4A (T37A,T46A,S65A,T70A) were plated in doxycycline containing media for 24 h. followed by methionine starvation for 30 min. Cells were then pulsed with L-Azidohomoalanine (AHA) for 2 h. (*D*). MCF7 cells were plated in 6 cm dishes and transfected with the depicted bicistronic luciferase construct containing the indicated 5′ UTR. Luciferase activity was measured after 24 h. n = 3 per group. *P*-values determined by ordinary one-way ANOVA. $P < 0.01$ indicated by **. (*E*). MCF7 cells were treated with 20 nM silvestrol for the indicated times. (*F*). MCF7 cells were starved of methionine for 30 min in the presence of MLN0128, silvestrol, or cycloheximide (50 μg/ml). Cells were then labeled with L-Azidohomoalanine (AHA) for 2 h. (*G*). MCF7 cells were transfected as in *D*, followed by treatment with increasing doses of silvestrol or MLN0128 for an additional 24 h. Luciferase activity was measured after 24 h. n = 3 per group.

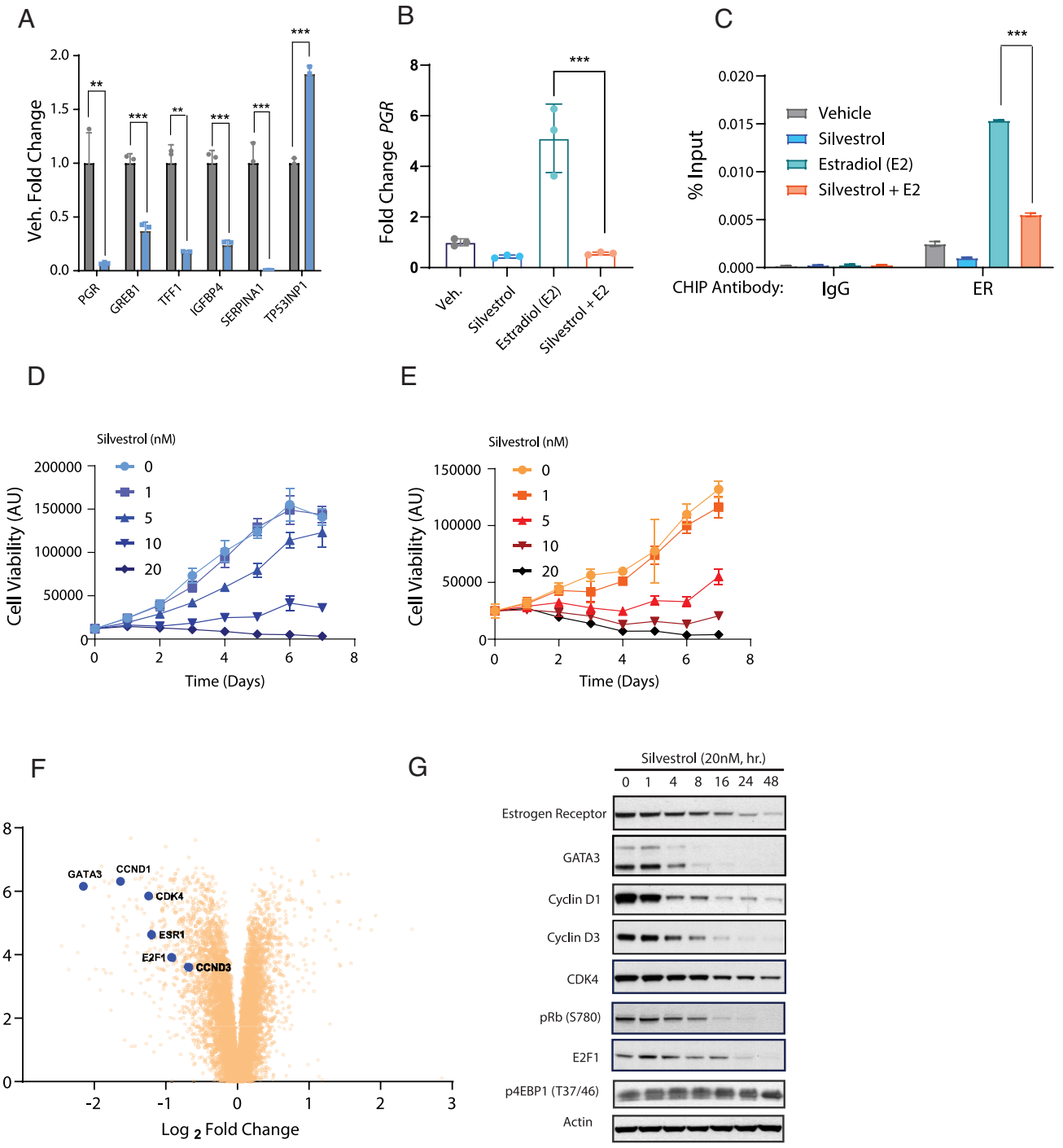

Fig. 2. eIF4A regulates ER activity and cell growth. (*A*) MCF7 cells were treated for 24 h. with 20 nM silvestrol followed by gene expression analysis by RT-qPCR. *P*-values were determined by students t test for each gene. n = 3 per group. $P < 0.01$ indicated as ** and $P < 0.001$ as ***. (*B*) MCF7 cells were plated in phenol red-free DMEM F12 containing charcoal stripped FBS followed by treatment with 20 nM silvestrol for 24 h. Cells were stimulated with 10 nM estradiol for an additional 24 h. *PGR* mRNA expression was analyzed by RT-qPCR. N = 3 per group. *P*-values were determined by ordinary one-way ANOVA. $P < 0.001$ is depicted as ***. (*C*) MCF7 cells were plated as in (*B*) followed by treatment with 20 nM silvestrol for 24 h. Cells were then stimulated with 10 nM estradiol for 1 h. ER binding to the *TFF1* enhancer element was analyzed by Chromatin Immunoprecipitation Assay (ChIP) and quantified by RT-qPCR. N = 3 per group. *P*-values were determined by ordinary one-way ANOVA within CHIP antibody groups. $P < 0.001$ is depicted as ***. (*D*) MCF7 cells were treated for up to 7 d with increasing doses of silvestrol. (*E*) T47D cells were treated for up to seven days with increasing doses of silvestrol. (*F*) MCF7 cells were treated with Veh. (DMSO) or silvestrol (20 nM) in triplicate for 24 h. Protein expression was analyzed by LC–MS.Significant hits were those proteins changing by at least log2 fold change>1and an adj. *P*-value of <0.05

expression. These data suggest that reducing ER expression by blocking eIF4A results in a decreased breast cancer response to estrogen in vitro. Silvestrol inhibited proliferation of ER-dependent MCF7 (Fig. 2*D*) and T47D (Fig. 2*E*) cells in a dose-dependent manner, with 5 nM reducing growth by 50% at 3 d and 20 nM halting growth completely over 7 d (Fig. 2 *D* and *E*). Therefore, eIF4A inhibition alone suppresses ER expression, downstream transcription, and proliferation of ER+ breast cancer cells.

Many transcripts have been described as sensitive to eIF4A inhibition, and eIF4A inhibitors can block the growth of various cancer models (39, 41, 46, 47). To identify global protein changes following eIF4A inhibition in our system, MCF7 cells were treated

with silvestrol (20 nM, 24 h) and analyzed by tandem mass tag (TMT) LC–MS proteomics (Fig. 2*F*). This facilitated the identification of proteins that are sensitive to eIF4A inhibition and that are short-lived enough to observe reduced expression after 24 h of treatment. We identified 122 proteins that were significantly reduced (≥2-fold), with several of relevance to ER+ breast cancer growth (Fig. 2*F* and Dataset S1). These included ER (ESR1) (>2-fold), ER cofactor GATA3 (~4-fold) (47), cell cycle regulators CDK4, E2F1, cyclin D3 (CCND3) (near twofold), and known eIF4A target cyclin D1 (CCND1) (40, 41). Immunoblot validation confirmed rapid decreases in ER, GATA3, cyclins D1 and D3, and CDK4, correlating with decreased Rb phosphorylation starting at 8 h (Fig. 2*G*). These findings establish that eIF4A inhibition suppresses ER-dependent gene expression and proliferation in ER+ breast cancers likely by regulating ER and G1 cyclins.

eIF4A Inhibition Combined with Fulvestrant Suppresses the Growth of ER+ Breast Cancer Models. In addition to being eIF4E and eIF4A dependently translated, cyclin D1 is also a well-established ER target gene (48). We hypothesized that combining an inhibitor of eIF4A with a Selective Estrogen Receptor Degrader (SERD) would further enhance the inhibition of ER and cyclin D1. MCF7 cells treated with the SERD, fulvestrant, showed a rapid reduction in ER protein levels, reaching a nadir at 4 h with partial recovery by 24 h (Fig. 3*A*). Silvestrol (20 nM) suppressed ER expression more slowly, beginning at 8 h and persisting through 24 h (Fig. 3*A*). The combination of both compounds suppressed ER expression fourfold more effectively than either compound alone (Fig. 3*A* and *SI Appendix*, Fig. S3*A*). Similar effects occurred in T47D cells, particularly at lower drug concentrations, with enhanced suppression of ER and cyclin D1 by combination treatment (*SI Appendix*, Fig. S3*B*). Using T47D cells expressing an ERE-driven luciferase reporter (49), low-dose silvestrol (5 nM), or fulvestrant (3 nM) individually blocked estradiol-stimulated activity, while their combination further reduced basal ER-driven expression by half (Fig. 3*B*). Higher doses (20 nM silvestrol, 30 nM fulvestrant) significantly lowered basal ER activity fivefold compared to untreated controls (Fig. 3*B*). Combination treatment was notably more effective at reducing estradiol-induced expression of target genes *PGR* and *TFF1/pS2* than either agent alone (*SI Appendix*, Fig. S3*C*). Combination treatment blocked cell growth in MCF7 and T47D approximately twice as effectively as either compound alone (Fig. 3*C* and *SI Appendix*, Fig. S3*D*). Consistent with their effects on cell cycle initiation, the combination also dramatically reduced the fraction of cells in S-phase (*SI Appendix*, Fig. S3*E*).

To test the effects of these inhibitors in vivo, we treated MCF7 xenografts with the bioavailable eIF4A inhibitor, CR-31-B (50), fulvestrant or the combination. We also used female mice implanted with either low (0.18 mg) or high (0.72 mg) estrogen pellets (Fig. 3 *D*–*G*). Under low estrogen conditions, fulvestrant alone effectively suppressed growth, while combination treatment induced mild regression (Fig. 3 *D* and *E*). Under high estrogen conditions, combination therapy led to significant, durable tumor regression lasting 45 d, superior suppression of ER and ER target proteins (progesterone receptor, GREB1), and markedly reduced Rb phosphorylation (Fig. 3 *F* and *G*). All treatments were well-tolerated, without observed weight loss (*SI Appendix*, Fig. S3*F*). Similar results were obtained when silvestrol was combined with other antiestrogens, including tamoxifen and elacestrant, as well as under estrogen-deprivation simulating conditions (*SI Appendix*, Fig. S3 *G*–*L*). Collectively, these data demonstrate combining eIF4A inhibitors with SERDs effectively reduces ER expression and tumor growth, while combination with SERMs also confers antiproliferative benefits, providing strong rationale for clinical development.

eIF4A Inhibition Blocks the Expression of Clinically Significant ER Variants. Resistance to antiestrogen therapies is often due to activating mutations in ER (51–53). Using MCF7 cells endogenously expressing the most common activating mutation, ER-D538G, we observed dose-dependent suppression of mutant ER and cyclin D1 by CR-31-B, saturating at 30 nM (Fig. 4*A*). Silvestrol similarly suppressed both wildtype and ER-D538G expression (*SI Appendix*, Fig. S4*A*). ER-D538G stability was similar to wildtype ER, with expression significantly reduced after 4 to 8 h of silvestrol treatment (*SI Appendix*, Fig. S4*B*). Consistent with previous data, ER-D538G cells exhibited reduced fulvestrant sensitivity (IC50 5.4 nM vs. 0.41 nM for wildtype) (*SI Appendix*, Fig. S4*C*). In contrast, both wild type and ER D538G mutant expressing cells were equally sensitive to CR-31-B (IC50 ~4 nM for both cell lines) (Fig. 4*C*).

To enhance suppression of cells expressing mutant ER, we tested CR-31-B combined with camizestrant, a newer SERD effective against ER mutants (54). Camizestrant (10 nM) or CR-31-B (3 nM) alone inhibited ER-D538G cell growth by ~70% at 7 d, while combination treatment further reduced growth by up to 95% (Fig. 4*C*). Camizestrant alone modestly suppressed ER and cyclin D1 expression. Suppression of both ER, but especially, cyclin D1 was enhanced when adding CR-31-B (3 nM) (Fig. 4*D*). CR-31-B (30 nM) fully suppressed cell growth and target protein expression, which in this case was not enhanced by camizestrant (Fig. 4*D*).

ER fusion proteins have recently been identified in breast cancer, and these have been shown to mediate acquired resistance to hormone receptor antagonists (55, 56). These variants are composed of the N-terminal portion of wildtype ER fused to a variety of C-terminal partners. The resulting constitutively active fusion protein lacks the hormone binding domain and cannot be inhibited by ER antagonists such as fulvestrant or tamoxifen. We generated T47D cells harboring an endogenously expressed ESR1–SOX9 fusion identified in clinical tumors (55, 56). (Fig. 4*E*). Cells expressing the ER–SOX9 fusion were enriched after selection in estrogen free media, thus confirming their estrogen independent growth (*SI Appendix*, Fig. S4*D*). In addition, the ER–SOX9 fusion could only be detected with an antibody against the N terminus but not the C-terminus of ER (*SI Appendix*, Fig. S4*D*). Fusion-expressing cells were markedly resistant to fulvestrant (GI50 ~10 μM vs. 10 nM for wildtype ER) (Fig. 4*F*). Treatment with CR-31-B (30 nM) reduced expression of the ER-SOX9 fusion and cyclin D1 levels below detection by 24 h (Fig. 4*G*). Wild type and fusion expressing cells were equally sensitive to CR-31-B, with GI50 values of approximately 4 nM (Fig. 4*H*). The half-life of the ER–SOX9 fusion was similar to that of wildtype ER, with significant suppression starting at 4 h post-silvestrol treatment and continuing thereafter (*SI Appendix*, Fig. S4*E*). Thus, ER variants associated with resistant to ER inhibitors remain sensitive to eIF4A inhibition.

Zotatifin + Fulvestrant Combination Lowers ER Expression and Suppresses Tumor Growth in Patients. The demonstration that expression of cell cycle regulators, and wild type, mutant, and ER fusion proteins are all sensitive to eIF4A inhibition suggests that it may be an effective clinical strategy, particularly in combination with standard endocrine therapies like fulvestrant that have relatively mild toxicity. Based on these results, early phase testing of the eIF4A inhibitor zotatifin (eFT226) included patients with ER+ metastatic breast cancer (MBC) (NCT04092673) (18). Similar to

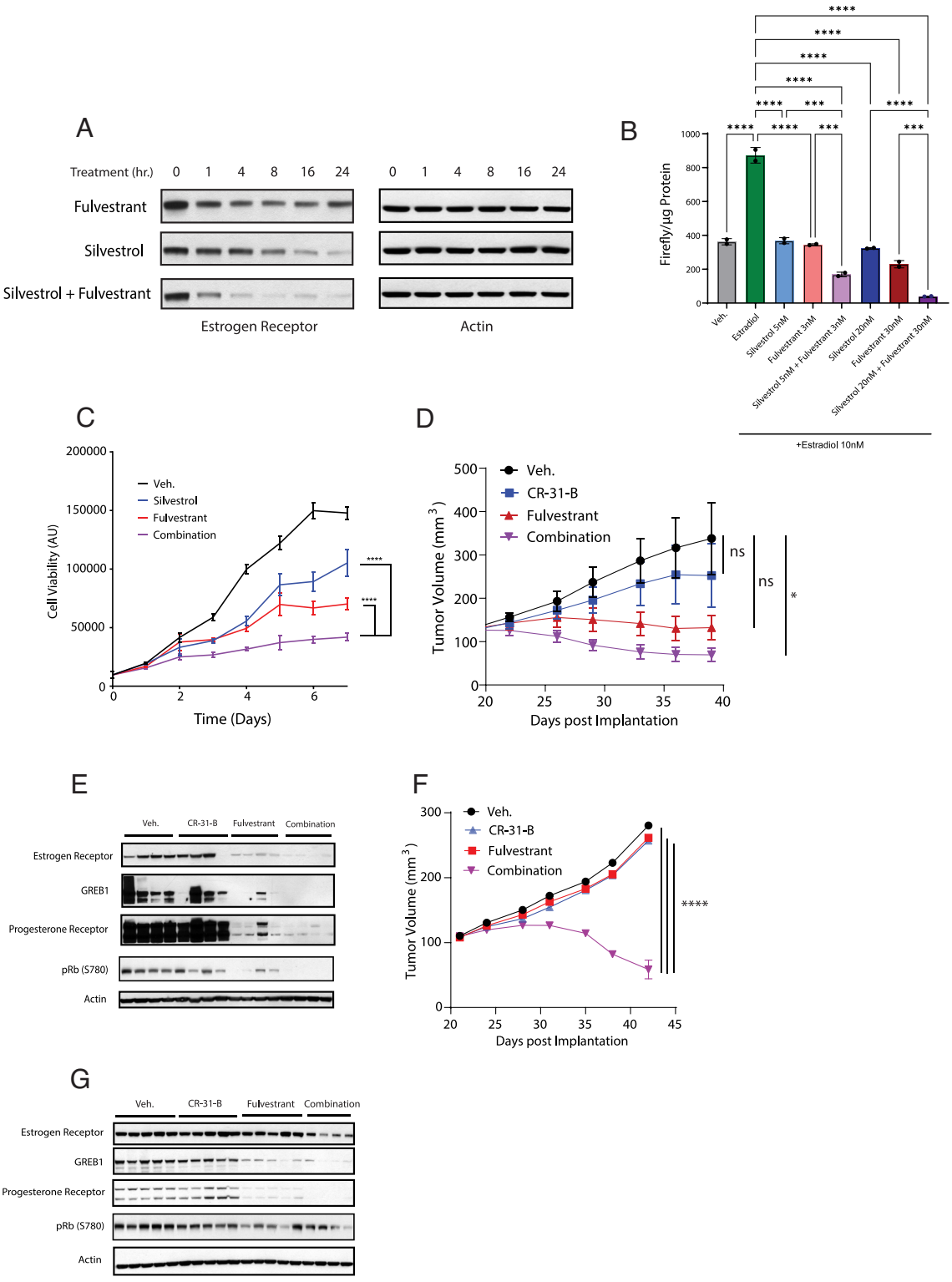

Fig. 3. eIF4A inhibition combined with fulvestrant suppresses the growth of ER+ breast cancer models. (*A*) MCF7 cells were treated for indicated times with Silvestrol (20 nM), Fulvestrant (30 nM), or the combination. (*B*) T47D-kBlue cells were plated in DMEM F12 containing charcoal stripped FBS and lacking phenol red, followed by treatment with the indicated doses of silvestrol or fulvestrant. Cells were then stimulated with 10 nM estradiol for an additional 24 h followed by luminescence quantification. The signal was normalized to protein mass. N = 2 replicates for each group. *P*-values were determined by ordinary one-way ANOVA. $P < 0.001$ is depicted as ***. $P < 0.0001$ is depicted as ****. (*C*) MCF7 cells were treated with either 5 nM silvestrol, 3 nM fulvestrant, or the combination for up to 7 d. N = 3 per group *P*-values were determined by ordinary one-way ANOVA at day seven. $P < 0.0001$ depicted as ****. (*D*) Nude mice were implanted with estrogen pellets (0.18 mg) for 3 d, followed by MCF7 xenograft implantation. Once tumors reached 100 mm^3, mice were treated twice weekly with 200 mg/kg Fulvestrant, 1 mg/kg CR-31-B, or the combination. N = 5 mice per group *P*-values were determined at the final time point by ordinary one-way ANOVA. $P < 0.05$ depicted as *. (*E*) Immunoblots from xenografts in Fig. 3*D* collected 24 h following the final dose of the indicated compounds. (*F*) Mice treated as in Fig. 3*D* but using 0.72 mg estrogen pellets. N = 5 per group, *P*-values were determined at the final time point by ordinary one-way ANOVA. $P < 0.0001$ depicted as ****. (*G*) Immunoblots from xenografts in figure 3*F* collected 24 h following the final dose of the indicated compounds.

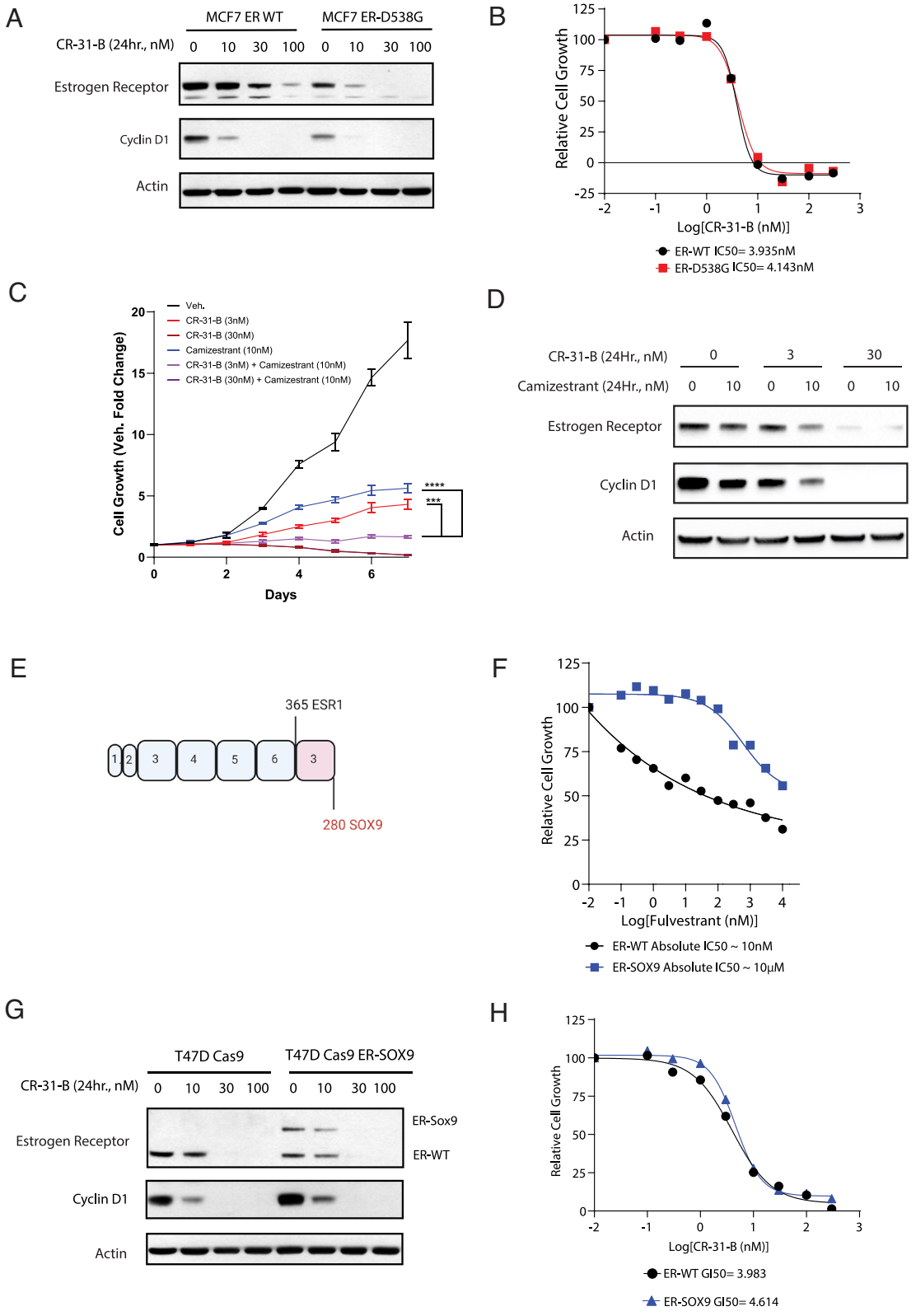

Fig. 4. eIF4A inhibition blocks expression of clinically significant ER variants. (*A*) MCF7 cells expressing either wild-type ER or ER-D538G were treated 24 h. with increasing doses of CR-31-B. (*B*) MCF7 cells expressing either wild-type ER or ER-D538G were treated 72 h. with increasing doses of CR-31-B. n = 3 per group. (*C*) MCF7 ER D538G cells were treated for up to 7 d with the indicated doses of Camizestrant, CR-31-B, or the combination. N = 3 per group *P*-values were determined by ordinary one-way ANOVA at day seven. $P < 0.001$ depicted as ***. $P < 0.0001$ depicted as ****. (*D*) MCF7 ER D538G were treated for 24 h. with the indicated doses of Camizestrant, CR-31-B or the combination. (*E*) Schematic showing the ESR1–SOX9 fusion protein. Exons and residues contributed by each protein are indicated. (*F*) T47D Cas9 and T47D Cas9 ESR1–SOX9 were treated for 72 h. with increasing doses of Fulvestrant. N = 3 per group. (*G*) T47D Cas9 or T47D Cas9 ESR1–SOX9 were treated for 24 h. with increasing doses of CR-31-B. (*H*) T47D Cas9 or T47D Cas9 ESR1–SOX9 were treated for 72 h. with increasing doses of CR-31-B. N = 3 per group.

other rocaglate eIF4A inhibitors such as silvestrol and CR-31-B, zotatifin forms an inhibitory tricomplex of the drug, eIF4A, and the 5' UTR of select mRNA (57) (Fig. 5*A*). Zotatifin is a first in class inhibitor of eIF4A and was designed by enhancing the physicochemical and pharmacokinetic properties of rocaglamide A (57) (Fig. 5*A*). Zotatifin was 10-fold less potent than silvestrol

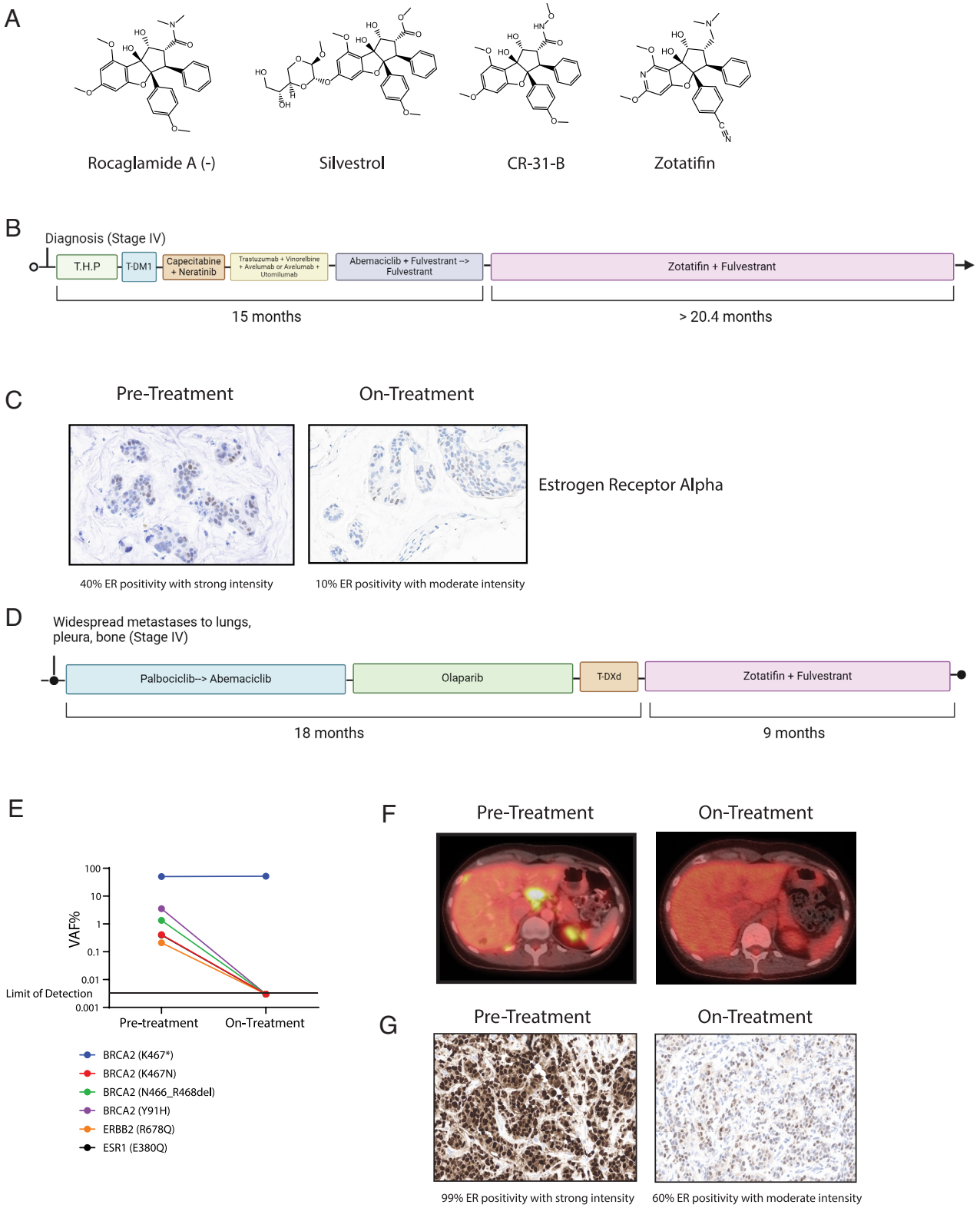

Fig. 5. Zotatifin + fulvestrant lowers ER expression and suppresses tumor growth in patients. (*A*) Chemical structures of various rocaglate inhibitors of eIF4A including clinical compound zotatifin. (*B*) Treatment timeline for patient 1. T.H.P = docetaxel, trastuzumab, and pertuzumab, TDM1 = Kadcyla (ado-trastuzumab emtansine). (*C*) IHC staining for Estrogen Receptor alpha pre- and on-treatment with Zotatifin + Fulvestrant. (*D*) Treatment timeline for patient 2. TDXD= Trastuzumab Deruxtecan. (*E*) Somatic cell–free DNA pre- and on-treatment with zotatifin + fulvestrant. (*F*) FDG PET CT showing pre- and on-treatment with zotatifin + fulvestrant. (*G*) IHC staining for Estrogen Receptor alpha pre- and on-treatment with Zotatifin + Fulvestrant.

and CR-31-B, requiring 100 nM to block ER and cyclin D1 expression and to fully inhibit cell growth (*SI Appendix*, Figs. S5 *A* and *B*). The ER+ metastatic breast cancer dose expansion cohort included two treatment arms: zotatifin + fulvestrant (ZF) and zotatifin + fulvestrant + abemaciclib (ZFA). Clinical responses were observed in heavily pretreated MBC patients in both the ZF and ZFA cohorts. On the ZF arm, 1/17 (5.9%) patients had a partial response. On the ZFA arm, 5/19 (26%) patients had partial responses (4 confirmed and 1 unconfirmed) and a median progression free-survival of 7.6 mo (18). All patients on the trial

have had previous exposure to and developed resistance to both fulvestrant and/or CDK4/6 inhibitors, suggesting that zotatifin both adds to combined endocrine + CDK4/6 inhibitor therapy and may potentially resensitize tumors with acquired resistance. Both ZF and ZFA regimens were well tolerated, with no dose-limiting toxicities or grade 5 adverse events (18).

Results thus far are consistent with our preclinical findings on the effects of combining inhibitors of eIF4A and ER. One patient treated on the ZF doublet arm (initially with ER+PR+HER2+ disease, subsequently with loss of HER2 positivity, likely with some degree of intratumoral HER2 heterogeneity) enrolled on the trial as 6th line therapy for progressive metastatic disease and experienced disease stability for over 19 mo, and continued on treatment at time of data cut (Fig. 5*B*). Analysis of pretreatment biopsies demonstrated ER expression by immunohistochemistry of 40%, while on-treatment biopsies showed near complete suppression of ER, with expression decreased to <10%. (Fig. 5*C*). A second patient in the ZF doublet arm enrolled on trial as 4th line therapy for progressive metastatic disease after receiving endocrine antiestrogen therapy + CDK4/6 inhibition, a PARP inhibitor, and the ADC trastuzumab deruxtecan in the metastatic setting (Fig. 5*D*). This patient had a brisk RECIST-confirmed partial response (–55%) at 8 wk, with regression of chest wall and liver lesions, as well as a 100% decline in somatic ctDNA 6 wk into treatment (Fig. 5 *E* and *F*). CtDNA analysis revealed a ESR1 E380Q (58) mutation and a somatic activating ERBB2 R678Q mutation, thereby providing proof of principle that these endocrine therapy-resistant subclones were sensitive to combination zotatifin therapy (Fig. 5*E*). While ER suppression at the protein level was not as complete as that seen in the first patient, pretreatment and on-treatment biopsies showed a significant change from >90% ER expression down to 60% (Fig. 5*G*). Overall, these data showing clinical responses coupled with this drug's well-tolerated side effect profile demonstrates that combination zotatifin therapy may represent a clinically viable strategy for treating metastatic ER+ breast cancer.

Discussion

In this work, we demonstrate that ER translation depends on eIF4A, and targeting eIF4A effectively inhibits ER expression and suppresses tumor growth in ER+ breast cancer. These findings indicate therapeutic potential, particularly in combination with well-tolerated endocrine therapies like fulvestrant and abemaciclib. This concept has been and will continue to be tested in clinical trials. Canonical eukaryotic translation is initiated by the m7G cap binding protein, eIF4E and is regulated by nutrient and growth factor-sensitive mTORC1 activity. During cellular stress certain mRNAs utilize cap-independent translation to sustain essential protein synthesis (15, 16, 33, 37, 59). Genes like Myc, Bcl-2, HIF1-alpha, c-jun, and Hox clusters utilize such mechanisms. *ESR1* is identified here as another example. Frequently, the elements mediating cap-independent translation are present in the transcript 5' untranslated region (5' UTR). Such elements are broadly termed, internal ribosome entry sites (IRESes) and often serve as binding sites for selectively employed initiation factors or to allow the ribosome to link directly with the mRNA transcript. IRESes often have complex 3D structures which require unwinding and remodeling during initiation, and eIF4A is one such protein employed for this purpose. G-quadraplex elements are one 3D structure that have been implicated in both cap-independent translation and in conferring eIF4A dependence to select mRNAs (41, 60). These elements are stable 3D arrangements of guanosines conjugating a monovalent cation (61). Indeed, the 5' UTR of ESR1 transcript variant 1 (NM_000125.4) is predicted to contain an abundance of overlapping and nonoverlapping G-quadraplex elements (62). Silvestrol, CR-31-B, and zotatifin have all been shown to block eIF4A-dependent unwinding of these structures (41, 63). Here, we demonstrate potential clinical applications of eIF4A-dependent ER regulation. Based on these findings, a clinical trial in ER+ breast cancer was initiated. Most patients had previously received antiestrogens and CDK4 inhibitors and became resistant. We showed clinical data from two patients in whom combination zotatifin and endocrine therapy was clinically active. These patients both show clear reduction in ER at the protein level. Activity of this combination may arise from the inhibition of several key proteins by nonoverlapping mechanisms. For instance, eIF4A and fulvestrant both inhibit ER and cyclin D1 by different mechanisms. Fulvestrant antagonizes and degrades ER while reducing mRNA expression of ER target genes such as cyclin D1. EIF4A inhibitors block translation of ER and G1 cyclins such as cyclin D1 and D3. This hypothesis is corroborated by the further efficacy enhancement of zotatifin + fulvestrant by adding the CDK4 inhibitor abemaciclib, which blocks cyclin D1–CDK4 complexes in yet a third way. It is also remarkable that the combination including a CDK4 inhibitor and an inhibitor of translation has only modest toxicity. This may depend on the important role of inhibiting the "driver" (ER) with a drug with low toxicity (fulvestrant) when combining with predictability more toxic agents such as eIF4A inhibitors. This strategy therefore may be applicable to the treatment of other tumors in which the oncoprotein drives D-cyclin expression, but for which allele-specific inhibitors exist, such as KRAS G12C or BRAF V600E. Taken together, these mechanistically informed clinical results demonstrate the utility of eIF4A inhibition in advanced breast cancer and predict rational potential for treating other solid tumors. Although the zotatifin triplet received an FDA fast track designation for treating metastatic breast cancer, during final preparations of this manuscript, the presiding company, eFFECTOR therapeutics which owned zotatifin lost sufficient liquidity to continue clinical development. This was exclusively due to internal managerial and strategic issues related to overall costs of pursuing several compounds simultaneously and was not related to any scientific, clinical efficacy, or safety concerns regarding zotatifin, or our collaborative findings. Other elements have expressed a high degree of interest in acquiring zotatifin and resuming its development as soon as possible.

Materials and Methods

Cell Culture and Treatments. All cell lines were purchased from American Type Culture Collection (ATCC). MCF7 (HTB-22), T47D (HTB-133), ZR-75-1 (CRL-1500), BT474 (HTB-20), SKOV3 (HTB-77), T47D-Kbluc (CRL-2865). All cell lines were maintained in DMEM/F12 supplemented with 10% Fetal Bovine Serum (FBS) and 1% penicillin and streptomycin. Stably generated cell lines including those expressing rtTA3 and tetracycline inducible constructs were maintained in DMEM/F12, 10% Tetracycline-free Fetal Bovine Serum (Tet-free FBS), and 1% penicillin and streptomycin. All cells were maintained in a humidified incubator with 5% CO_2 at 37 °C. Silvestrol and CR-1-31-B (CR-31-B) were obtained from the Wendel lab and organic synthesis core at MSK. Zotatifin was provided by eFFECTOR therapeutics. Fulvestrant (HY-13636), tamoxifen (HY-13757A), elacestrant (HY-19822), and camizestrant (HY-136255) were purchased from Medchemexpress. Charcoal stripped FBS and DMEM/F-12 lacking phenol red were purchased from Gibco. RapaLink-1 was obtained from ongoing collaborations with the Shokat lab at UCSF. All compounds were dissolved in DMSO, and DMSO was used in all cases as a vehicle control.

Immunoblotting. Cells were collected in ice-cold PBS and lysed with 1X RIPA buffer supplemented with protease and phosphatase inhibitors. Lysates were briefly sonicated before centrifugation at 20,000×*g* for 5 min at 4 °C. The supernatant was collected, and protein concentration was quantified using BCA. Equal amounts of protein (20 μg) in cell lysates were separated by SDS–PAGE,

transferred to nitrocellulose membranes (GE healthcare), probed with specific primary and secondary antibodies, and detected by chemiluminescence with the ECL detection reagents from Thermo Fisher or Millipore.

Quantification of Cell Growth and Viability. Cells were seeded into 96-well plates at a density of 2,000 to 5,000 cells per well. Cell growth was quantified using the CellTiter-Glo assay from Promega. For each condition, at least 3 replicates were measured.

Study of eFT226 (Zotatifin) in Subjects with Selected Advanced Solid Tumor Malignancies. This was a US, open-label, phase 1 to 2 Dose-Escalation and Cohort-Expansion Study of Intravenous Zotatifin (eFT226) in Subjects With Selected Advanced Solid Tumor Malignancies (NCT04092673). The study was conducted in accordance with the Declaration of Helsinki and was reviewed and approved by the Memorial Sloan Kettering institutional review board (MSK-IRB #21-323). Written informed consent was obtained from all patients before study entry. Patients eligible for study participation were ≥18 y old, had histological or cytological confirmation of breast cancer, metastatic disease, or locoregionally recurrent disease which is refractory or intolerant to existing therapy(ies) known to provide clinical benefit, and prior treatment had included a CDK4/6 inhibitor. For purposes of this paper, cutoff for clinical data collection was June 30, 2024.

Statistical Analysis. The details of statistical analysis of experiments can be found in the figure legends. All data were plotted as mean ± SD with the exception of Fig. 3 *D* and *F* which were plotted as mean ± SEM. Statistical analysis of differences between two groups was performed using two-tailed Student's *t* test, and $P < 0.05$ was defined as significant. One-way ANOVA was performed to compare the means of more than two groups. All analyses were conducted using GraphPad Prism 8.0.

Data, Materials, and Software Availability. All study data are included in the article and/or supporting information.

ACKNOWLEDGMENTS. We are grateful to Priya Pancholi for her assistance with the experiments, and all members of the Rosen and Chandarlapaty labs past and present for helpful discussions and advice. Thanks to Ventura lab for help with CRISPR experiments. NCI Core Grant P30 CA008748 is gratefully acknowledged for partial funding of both the Organic Synthesis and Mouse Pharmacology Core Facilities at MSKCC. The Organic Synthesis Core is also partially funded through NCI Grant R50 CA243895. F. Pareja is funded in part by an NIH/NCI P50 CA24779 01 Grant and by a Starr Cancer Consortium Grant. The Wendel lab gratefully acknowledges funding from R35 CA252982, Harrington Discovery Institute's 2022 Scholar Innovator Award, Starr Technology Commercialization Fund (Starr TCF) and P30 CA008748. S. Chandarlapaty is supported by NIH Cancer Center Support Grant P30-CA008748 and NIH R01CA245069 and the BCRF. This research was supported by grants (to N.R.) (and long term support from the BCRF) from the NIH P01-CA129243; R35 CA210085; the Geoffrey Beene Cancer Research Center; the Emerson Collective Research Grant, The NIH MSKCC Cancer Center Core Grant P30 CA008748 and Experimental Therapeutics Center. We thank Dr. Nahum Sonenberg for providing the pcDNA3 RLUC POLIRES FLUC plasmid (Addgene plasmid #45642). All illustrations were designed with BioRender, and all chemical structures were designed with ChemDraw.

Author affiliations: [a]Louis V. Gerstner Jr. Graduate School of Biomedical Sciences, Memorial Sloan Kettering Cancer Center, New York, NY 10065; [b]Program in Molecular Pharmacology, Department of Medicine, Memorial Sloan Kettering Cancer Center, New York, NY 10065; [c]Ludwig Institute for Cancer Research, Princeton Branch, Princeton, NJ 08544; [d]Department of Medicine, Memorial Sloan Kettering Cancer Center, New York, NY 10065; [e]Human Oncology and Pathogenesis Program, Memorial Sloan Kettering Cancer Center, New York, NY 10065; [f]Department of Cancer Biology and Genetics, Sloan Kettering Institute, Memorial Sloan Kettering Cancer Center, New York, NY 10065; [g]Microchemistry and Proteomics Core Facility, Memorial Sloan Kettering Cancer Center, New York, NY 10065; [h]Antitumor Assessment Core Facility, Memorial Sloan Kettering Cancer Center, New York, NY 10065; [i]Department of Pathology and Laboratory Medicine, Memorial Sloan Kettering Cancer Center, New York, NY 10065; [j]Department of Cancer Biology, eFFECTOR Therapeutics, Inc., San Diego, CA 92121; [k]The Organic Synthesis Core Facility, Memorial Sloan Kettering Cancer Center, New York, NY 10065; and [l]Department of Medicine, Weill Cornell Medicine, New York, NY 10065

1. J. R. Tata, Signalling through nuclear receptors. *Nat. Rev. Mol. Cell Biol.* **3**, 702–710 (2002).
2. J. S. Carroll *et al.*, Genome-wide analysis of estrogen receptor binding sites. *Nat. Genet.* **38**, 1289–1297 (2006).
3. C. J. Watson, W. T. Khaled, Mammary development in the embryo and adult: New insights into the journey of morphogenesis and commitment. *Development* **147**, dev169862 (2020).
4. H. S. Rugo *et al.*, Endocrine therapy for hormone receptor-positive metastatic breast cancer: American Society of Clinical Oncology guideline. *J. Clin. Oncol.* **34**, 3069–3103 (2016).
5. D. Musheyev, A. Alayev, Endocrine therapy resistance: What we know and future directions. *Explor. Target. Anti-Tumor Ther.* **3**, 480–496 (2022).
6. J. W. Chen *et al.*, Comparison of *PIK3CA* mutation prevalence in breast cancer across predicted ancestry populations. *JCO Precis. Oncol.* **6**, e2200341 (2022).
7. J. Gao *et al.*, Integrative analysis of complex cancer genomics and clinical profiles using the cBioPortal. *Sci. Signal.* **6**, pl1 (2013).
8. E. Cerami *et al.*, The cBio cancer genomics portal: An open platform for exploring multidimensional cancer genomics data. *Cancer Discov.* **2**, 401–404 (2012).
9. R. A. Saxton, D. M. Sabatini, mTOR signaling in growth, metabolism, and disease. *Cell* **168**, 960–976 (2017).
10. N. Sonenberg, A. G. Hinnebusch, Regulation of translation initiation in eukaryotes: Mechanisms and biological targets. *Cell* **136**, 731–745 (2009).
11. A. Bosch *et al.*, PI3K inhibition results in enhanced estrogen receptor function and dependence in hormone receptor–positive breast cancer. *Sci. Transl. Med.* **7**, 283ra51 (2015).
12. E. Toska *et al.*, PI3K pathway regulates ER-dependent transcription in breast cancer through the epigenetic regulator KMT2D. *Science* **355**, 1324–1330 (2017).
13. C. C. Thoreen *et al.*, A unifying model for mTORC1-mediated regulation of mRNA translation. *Nature* **485**, 109–113 (2012).
14. A.-C. Godet *et al.*, IRES trans-acting factors, key actors of the stress response. *Int. J. Mol. Sci.* **20**, 924 (2019).
15. R. J. Jackson, S. L. Hunt, J. E. Reynolds, A. Kaminski, Cap–independent translation. *Curr Top Microbiol* **203**, 1–29 (2011).
16. I. N. Shatsky, I. M. Terenin, V. V. Smirnova, D. E. Andreev, Cap-independent translation: What's in a name? *Trends Biochem. Sci.* **43**, 882–895 (2018).
17. A. M. Nardulli, B. S. Katzenellenbogen, Dynamics of estrogen receptor turnover in uterine cells in vitro and in uteri in vivo. *Endocrinology* **119**, 2038–2046 (1986).
18. E. Rosen *et al.*, Phase 1/2 dose expansion study evaluating first-in-class eIF4A inhibitor zotatifin in patients with ER+ metastatic breast cancer. *J. Clin. Oncol.* **41**, 1080–1080 (2023).
19. R. J. Jackson, C. U. T. Hellen, T. V. Pestova, The mechanism of eukaryotic translation initiation and principles of its regulation. *Nat. Rev. Mol. Cell Biol.* **11**, 113–127 (2010).
20. J. Pelletier, N. Sonenberg, The organizing principles of eukaryotic ribosome recruitment. *Annu. Rev. Biochem.* **88**, 307–335 (2019).
21. S. Grüner *et al.*, The structures of eIF4E-eIF4G complexes reveal an extended interface to regulate translation initiation. *Mol. Cell* **64**, 467–479 (2016).
22. A.-C. Gingras, B. Raught, N. Sonenberg, Regulation of translation initiation by FRAP/mTOR. *Genes Dev.* **15**, 807–826 (2001).
23. G. W. Rogers, A. A. Komar, W. C. Merrick, eIF4A: The godfather of the DEAD box helicases. *Prog Nucleic Acid Re* **72**, 307–331 (2002).
24. A. Parsyan *et al.*, mRNA helicases: The tacticians of translational control. *Nat. Rev. Mol. Cell Biol.* **12**, 235–245 (2011).
25. S. Chandarlapaty *et al.*, Akt inhibition relieves feedback suppression of receptor tyrosine kinase expression and activity. *Cancer Cell* **19**, 58–71 (2011).
26. T. Muranen *et al.*, Inhibition of PI3K/mTOR leads to adaptive resistance in matrix-attached cancer cells. *Cancer Cell* **21**, 227–239 (2012).
27. V. S. Rodrik-Outmezguine *et al.*, Overcoming mTOR resistance mutations with a new-generation mTOR inhibitor. *Nature* **534**, 272–276 (2016).
28. R. J. O. Dowling *et al.*, *mTORC1*-mediated cell proliferation, but not cell growth, controlled by the 4E-BPs. *Science* **328**, 1172–1176 (2010).
29. J. Averous, B. D. Fonseca, C. G. Proud, Regulation of cyclin d1 expression by mTORC1 signaling requires eukaryotic initiation factor 4E-binding protein 1. *Oncogene* **27**, 1106–1113 (2008).
30. L. Philippe, A. M. G. van den Elzen, M. J. Watson, C. C. Thoreen, Global analysis of LARP1 translation targets reveals tunable and dynamic features of 5′ TOP motifs. *Proc. Natl. Acad. Sci. U.S.A.* **117**, 5319–5328 (2020).
31. P. Landgraf, E. R. Antileo, E. M. Schuman, D. C. Dieterich, Site-specific protein labeling, methods and protocols. *Methods Mol. Biol.* **1266**, 199–215 (2014).
32. A.-C. Gingras, S. G. Kennedy, M. A. O'Leary, N. Sonenberg, N. Hay, 4E-BP1, a repressor of mRNA translation, is phosphorylated and inactivated by the Akt(PKB) signaling pathway. *Genes Dev.* **12**, 502–513 (1998).
33. M. Stoneley *et al.*, C-myc protein synthesis is initiated from the internal ribosome entry segment during apoptosis. *Mol. Cell. Biol.* **20**, 1162–1169 (2000).
34. K. A. Spriggs, M. Stoneley, M. Bushell, A. E. Willis, Re-programming of translation following cell stress allows IRES-mediated translation to predominate. *Biol. Cell* **100**, 27–38 (2008).
35. T. E. Graber, M. Holcik, Cap-independent regulation of gene expression in apoptosis. *Mol. Biosyst.* **3**, 825–834 (2007).
36. F. Poulin, A.-C. Gingras, H. Olsen, S. Chevalier, N. Sonenberg, 4E-BP3, a new member of the eukaryotic initiation factor 4E-binding protein family*. *J. Biol. Chem.* **273**, 14002–14007 (1998).
37. K. Leppek, R. Das, M. Barna, Functional 5′ UTR mRNA structures in eukaryotic translation regulation and how to find them. *Nat. Rev. Mol. Cell Biol.* **19**, 158–174 (2018).
38. A. G. Hinnebusch, Molecular mechanism of scanning and start codon selection in eukaryotes. *Microbiol. Mol. Biol. Rev.* **75**, 434–467 (2011).
39. J. Chu *et al.*, Amidino-rocaglates: A potent class of eIF4A inhibitors. *Cell Chem. Biol.* **26**, 1586–1593.e3 (2019).
40. L. Alinari *et al.*, Dual targeting of the cyclin/Rb/E2F and mitochondrial pathways in mantle cell lymphoma with the translation inhibitor silvestrol. *Clin. Cancer Res.* **18**, 4600–4611 (2012).
41. A. L. Wolfe *et al.*, RNA G-quadruplexes cause eIF4A-dependent oncogene translation in cancer. *Nature* **513**, 65–70 (2014).
42. C. M. Rodrigo, R. Cencic, S. P. Roche, J. Pelletier, J. A. Porco, Synthesis of rocaglamide hydroxamates and related compounds as eukaryotic translation inhibitors: Synthetic and biological studies. *J. Med. Chem.* **55**, 558–562 (2012).

43. J. Steinberger *et al.*, Identification and characterization of hippuristanol-resistant mutants reveals eIF4A1 dependencies within mRNA 5′ leader regions. *Nucleic Acids Res.* **48**, gkaa662- (2020).
44. S. K. Naineni *et al.*, A comparative study of small molecules targeting eIF4A. *RNA* **26**, 541–549 (2020), 10.1261/rna.072884.119.
45. J. Guan *et al.*, Therapeutic ligands antagonize estrogen receptor function by impairing its mobility. *Cell* **178**, 949–963.e18 (2019), 10.1016/j.cell.2019.06.026.
46. Y. Nishida *et al.*, Inhibition of translation initiation factor eIF4A inactivates heat shock factor 1 (HSF1) and exerts anti-leukemia activity in AML. *Leukemia* **35**, 2469–2481 (2021).
47. K. Singh *et al.*, Targeting eIF4A-dependent translation of KRAS signaling molecules. *Cancer Res.* **81**, 2002–2014 (2021).
48. M. Sabbah, D. Courilleau, J. Mester, G. Redeuilh, Estrogen induction of the cyclin D1 promoter: Involvement of a cAMP response-like element. *Proc. Natl. Acad. Sci. U.S.A.* **96**, 11217–11222 (1999).
49. V. S. Wilson, K. Bobseine, L. E. Gray, Development and characterization of a cell line that stably expresses an estrogen-responsive luciferase reporter for the detection of estrogen receptor agonist and antagonists. *Toxicol. Sci.* **81**, 69–77 (2004).
50. Y. Cao, Y. He, L. Yang, Z. Luan, Targeting eIF4A using rocaglate CR-1-31B sensitizes gallbladder cancer cells to TRAIL-mediated apoptosis through the translational downregulation of c-FLIP. *Oncol. Rep.* **45**, 230–238 (2021).
51. J. A. Katzenellenbogen, C. G. Mayne, B. S. Katzenellenbogen, G. L. Greene, S. Chandarlapaty, Structural underpinnings of oestrogen receptor mutations in endocrine therapy resistance. *Nat. Rev. Cancer* **18**, 377–388 (2018).
52. C. X. Ma, T. Reinert, I. Chmielewska, M. J. Ellis, Mechanisms of aromatase inhibitor resistance. *Nat. Rev. Cancer* **15**, 261–275 (2015).
53. S. Irani *et al.*, Somatic estrogen receptor α mutations that induce dimerization promote receptor activity and breast cancer proliferation. *J. Clin. Invest.* **134**, e163242 (2023).
54. M. Lawson *et al.*, The next-generation oral selective estrogen receptor degrader camizestrant (AZD9833) suppresses ER+ breast cancer growth and overcomes endocrine and CDK4/6 inhibitor resistance. *Cancer Res.* **83**, 3989–4004 (2023).
55. J. T. Lei *et al.*, Functional annotation of *ESR1* gene fusions in estrogen receptor-positive breast cancer. *Cell Rep.* **24**, 1434–1444.e7 (2018).
56. R. J. Hartmaier *et al.*, Recurrent hyperactive ESR1 fusion proteins in endocrine therapy-resistant breast cancer. *Ann. Oncol.* **29**, 872–880 (2018).
57. J. T. Ernst *et al.*, Design of development candidate eFT226, a first in class inhibitor of eukaryotic initiation factor 4A RNA helicase. *J. Med. Chem.* **63**, 5879–5955 (2020).
58. Y. Kuang *et al.*, Unraveling the clinicopathological features driving the emergence of *ESR1* mutations in metastatic breast cancer. *NPJ Breast Cancer* **4**, 22 (2018).
59. I. M. Terenin, V. V. Smirnova, D. E. Andreev, S. E. Dmitriev, I. N. Shatsky, A researcher's guide to the galaxy of IRESs. *Cell. Mol. Life Sci.* **74**, 1431–1455 (2017).
60. M. J. Morris, Y. Negishi, C. Pazsint, J. D. Schonhoft, S. Basu, An RNA G-quadruplex is essential for cap-independent translation initiation in human VEGF IRES. *J. Am. Chem. Soc.* **132**, 17831–17839 (2010).
61. C. K. Kwok, M. E. Sherlock, P. C. Bevilacqua, Effect of loop sequence and loop length on the intrinsic fluorescence of G-quadruplexes. *Biochemistry* **52**, 3019–3021 (2013).
62. O. Kikin, L. D'Antonio, P. S. Bagga, QGRS Mapper: A web-based server for predicting G-quadruplexes in nucleotide sequences. *Nucleic Acids Res.* **34**, W676–W682 (2006).
63. E. Horvilleur *et al.*, Cap-in-dependent translation in hematological malignancies. *Front. Oncol.* **5**, 293 (2015).